

University of Windsor

## Scholarship at UWindor

---

Electronic Theses and Dissertations

Theses, Dissertations, and Major Papers

---

1-10-2024

# NOVEL APPROACHES TO FAST OCV CHARACTERIZATION AND IMPROVED CAPACITY ESTIMATION IN LITHIUM ION BATTERIES

James Vu Nguyen  
*University of Windsor*

Follow this and additional works at: <https://scholar.uwindsor.ca/etd>



Part of the [Engineering Commons](#)

---

### Recommended Citation

Nguyen, James Vu, "NOVEL APPROACHES TO FAST OCV CHARACTERIZATION AND IMPROVED CAPACITY ESTIMATION IN LITHIUM ION BATTERIES" (2024). *Electronic Theses and Dissertations*. 9147. <https://scholar.uwindsor.ca/etd/9147>

This online database contains the full-text of PhD dissertations and Masters' theses of University of Windsor students from 1954 forward. These documents are made available for personal study and research purposes only, in accordance with the Canadian Copyright Act and the Creative Commons license—CC BY-NC-ND (Attribution, Non-Commercial, No Derivative Works). Under this license, works must always be attributed to the copyright holder (original author), cannot be used for any commercial purposes, and may not be altered. Any other use would require the permission of the copyright holder. Students may inquire about withdrawing their dissertation and/or thesis from this database. For additional inquiries, please contact the repository administrator via email ([scholarship@uwindsor.ca](mailto:scholarship@uwindsor.ca)) or by telephone at 519-253-3000ext. 3208.

**NOVEL APPROACHES TO FAST OCV CHARACTERIZATION AND  
IMPROVED CAPACITY ESTIMATION IN LITHIUM ION  
BATTERIES**

by

James Nguyen

A Thesis  
Submitted to the Faculty of Graduate Studies  
through the Department of Electrical and Computer Engineering  
in Partial Fulfilment of the Requirements for  
the Degree of Master of Applied Science at the  
University of Windsor

Windsor, Ontario, Canada

© 2023 James Nguyen

NOVEL APPROACHES TO FAST OCV CHARACTERIZATION AND  
IMPROVED CAPACITY ESTIMATION IN LITHIUM ION BATTERIES

by  
James Nguyen

APPROVED BY:

---

Y. Kim  
Department of Civil & Environmental Engineering

---

S. Chowdhury  
Department of Electrical and Computing Engineering

---

B. Balasingam, Advisor  
Department of Electrical and Computing Engineering

December 11, 2023

# Declaration of Co-Authorship / Previous Publication

## Co-Authorship

I hereby declare that this thesis incorporates material that is result of joint research, as follows: Chapter 2 and 3 of this thesis were co-authored by P. Pillai and Dr. B. Balasingam Chapters 2 and 3 of the thesis include the outcome of publications which have the following other co-authors: P. Pillai and Dr. B. Balasingam. In all cases only my primary contributions towards these publications are included in this thesis, and the contribution of co-authors was primarily through assistance in experimentation and analysis of previous ideas.

In all cases, the key ideas, primary contributions, experimental designs, data analysis, interpretation, and writing were performed by me. I am aware of the University of Windsor Senate Policy on Authorship and I certify that I have properly acknowledged the contribution of other researchers to my thesis, and have obtained written permission from each of the co-author(s) to include the above material(s) in my thesis.

## Previous Publication

Thesis chapter	Publication title/full citation	Publication status	Journal
2	J. Nguyen, P. Pillai, and B. Balasingam, "A Fast OCV Characterization Approach for Battery reuse Applications," in 2022 IEEE Electrical Power and Energy Conference (EPEC), pp. 194–199, 2022	Published	2022 IEEE Electrical Power and Energy Conference
3	J. Nguyen, P. Pillai, and B. Balasingam, "Offsetting Approach for Capacity Estimation in Li-ion Batteries"	In progress	TBD

I certify that I have obtained a written permission from the copyright owner(s) to include the above published material(s) in my thesis. I certify that the above material describes work completed during my registration as a graduate student at the University of Windsor.

## General

I declare that, to the best of my knowledge, my thesis does not infringe upon anyone's copyright nor violate any proprietary rights and that any ideas, techniques, quotations, or any other material from the work of other people included in my thesis, published or otherwise, are fully acknowledged in accordance with the standard referencing practices. Furthermore, to the extent that I have included copyrighted material that surpasses the bounds of fair dealing within the meaning of the Canada Copyright Act, I certify that I have obtained a written permission from the copyright owner(s) to include such material(s) in my thesis. I declare that this is a true copy of my thesis, including any final revisions, as approved by my thesis committee and the Graduate Studies office, and that this thesis has not been submitted for a higher degree to any other University or Institution.

# Abstract

This thesis considers the problem of open circuit voltage (OCV) to state of charge (SOC) characterization in li-ion batteries for battery reuse applications. The traditional approach to OCV-SOC characterization is done by collecting voltage and current data through a slow discharge and charge process; this process usually takes about 60 hours. Such OCV-SOC characterization is performed on a few sample batteries because the OCV-SOC characterization is considered to be the same for new batteries coming out of the same manufacturing process. However, the characteristics of a battery may change as it is used for years in different environmental and usage conditions. Hence, they may need to be re-characterized before secondary use. Unlike primary characterization, the secondary characterization may have to be done faster in order to save time and cost. This thesis presents a faster approach for OCV-SOC characterization. The proposed approach in this thesis consists of constant-current profiles that halves in magnitude after a specified time. Such reductions allows us to fully deplete the battery; similarly, the battery is charged back with a reducing current profile in order to make sure the battery is fully charged. The resulting current profile reduces the total characterization time by  $1/5$ . Secondly, we explore the idea of discharge and charge capacity of batteries. A traditional low-rate-OCV test consists of constant-current charging which results in a voltage drop based on the internal resistance and charging/discharging current. This thesis presents an approach to counteract this voltage drop, by appropriately over-charging and over-discharging the battery to obtain the most accurate representation of the capacity of the battery.

# Contents

<b>Declaration of Co-Authorship / Previous Publication</b>	<b>iii</b>
<b>Abstract</b>	<b>v</b>
<b>List of Tables</b>	<b>viii</b>
<b>List of Figures</b>	<b>ix</b>
<b>1 Introduction</b>	<b>1</b>
1.1 Organization of the Thesis . . . . .	3
1.2 Bibliography . . . . .	4
<b>2 A Fast OCV Characterization Approach for Battery Reuse Applications</b>	<b>5</b>
2.1 Introduction . . . . .	6
2.2 OCV Modeling Approaches . . . . .	7
2.2.1 Traditional OCV modelling approach . . . . .	7
2.2.2 OCV Modelling Through Averaging . . . . .	11
2.3 Charging Strategies for OCV test . . . . .	13
2.3.1 Characterization approach (Slow Method) . . . . .	13
2.3.2 Characterization approach (Fast Method) . . . . .	14
2.4 Performance metrics . . . . .	15
2.5 Experimental Details . . . . .	16

2.6	Results . . . . .	16
2.7	Conclusions . . . . .	20
2.8	Bibliography . . . . .	21
<b>3</b>	<b>Offsetting Approach for Capacity Estimation in Li-ion Batteries</b>	<b>24</b>
3.1	Introduction . . . . .	25
3.2	Voltage Difference . . . . .	27
3.3	Battery Cycling . . . . .	27
3.4	Low-Rate-OCV-Test (N) . . . . .	28
3.5	Value of $V_d$ at different OCV rates . . . . .	28
3.6	Experimental Details . . . . .	28
3.6.1	Data Collection System . . . . .	29
3.6.2	Batteries . . . . .	30
3.6.3	Voltage-Current Data . . . . .	31
3.6.4	Analyzing the OCV curve . . . . .	32
3.6.5	Battery Voltage Drop . . . . .	35
3.7	Computation of Comparison Metrics . . . . .	35
3.7.1	Computing the Battery Capacity . . . . .	36
3.8	Results . . . . .	37
3.9	Conclusions . . . . .	40
3.10	Bibliography . . . . .	40
<b>4</b>	<b>Thesis Conclusion</b>	<b>42</b>
	<b>Vita Auctoris</b>	<b>43</b>



# List of Tables

2.1	Pairs of OCV-SOC values . . . . .	12
2.2	Capacities of both charging methods Slow vs. Fast . . . . .	18
2.3	Internal resistances of all 4 cells at different SOCs . . . . .	19
3.4	$V_d$ at different OCV rates . . . . .	29
3.5	Specifications of Li-ion battery. . . . .	30
3.6	List of complete data collection . . . . .	31
3.7	Battery capacity estimates calculated at different C-Rates . . . . .	38
3.8	Average charge and discharge capacity for both approaches . . . . .	39

# List of Figures

2.1	<b>DC equivalent circuit model.</b> . . . . .	8
2.2	An estimate of OCV is calculated by averaging $\hat{V}_o'(k)$ over a window of the length $T_w$ . . . . .	12
2.3	<b>Fast Charge collection plan tested during the experiment as well as the expected SOC after each step</b> . . . . .	14
2.4	Experimental setup for battery testing [13] . . . . .	16
2.5	The current profile recorded for all four batteries is shown here. The traditional OCV test is followed by the fast OCV characterization test. . . . .	17
2.6	The current profile recorded for the fast characterization method is shown here. . . . .	17
2.7	OCV-SOC curves estimated for all four batteries using the Combined+3 model. . . . .	18
2.8	OCV error obtained through the difference in voltages between the true voltage (slow method) compared to the fast OCV characterization using the traditional OCV modelling approach (Fast OCV - I). . . . .	19
2.9	OCV error obtained through the difference in voltages between the true voltage (slow method) compared to the Fast OCV characterization using the OCV modelling through the averaging approach (Fast OCV - II). . . . .	20
3.10	Arbin battery cycler. . . . .	29
3.11	Molicel INR-21700-P42A batteries. . . . .	30

3.12 Low-rate OCV characterization data collected at the C/2 and C/128 rate. . . . .	33
3.13 Terminal Voltage Comparison . . . . .	33
3.14 Generic OCV model . . . . .	34
3.15 Charge/Discharge and Average OCV curve . . . . .	34
3.16 <b>DC equivalent circuit model.</b> . . . . .	35
3.17 Charge Capacity Comparison . . . . .	39
3.18 Discharge Capacity Comparison . . . . .	39
3.19 Charge and Discharge Capacity visual for both cases . . . . .	39

# Chapter 1

## Introduction

Li-ion batteries play a pivotal role in the landscape of hybrid and electric vehicles today, standing as the linchpin technology that propels the sustainable mobility revolution forward. The importance of these batteries lie in their exceptional energy density, longevity, and re-chargeability, which enable vehicles to achieve extended all-electric ranges and overall enhanced fuel efficiency. Their ongoing advancements in terms of cost reduction and performance improvements continue to reshape the automotive industry, accelerating the global shift towards eco-friendly transportation alternatives. For safety reasons, these li-ion battery pack need to be managed in order to ensure the safety, dependability, and effectiveness of these batteries. A Battery Management System (BMS) is responsible for overseeing the present flow, temperature, and instantaneous voltage of the batteries while also executing various corrective actions as described by [1]. The BMS operates by implementing corrective measures to guarantee safety, relying on estimations of vital battery parameters including impedance, State-of-Charge (SOC), capacity, State-of-Health (SOH), time to shut down, and remaining useful lifespan.

Battery reuse is one of the growing concerns in our world today. For instance, battery packs of EVs that are not used anymore can be reused for different applications such as energy storage systems, grid stabilization, and off-grid applications after the

end of life of the EV. As of now, there are two routes for a battery at its end-of-life: reuse or recycle. Currently, battery recycling is most prevalent as compared to reuse primarily to re-obtain materials such as lithium, cobalt, and nickel to manufacture new batteries. This process can be extremely long and the effort may not be worth the gain. Also, recycling consumes a lot of energy. It makes more environmental sense to reuse before recycling. To know if a battery can be reused, a full characterization of the battery needs to be obtained to evaluate battery degradation. A traditional characterization currently takes around 60 hours to obtain necessary parameters and this is not feasible when hundreds of batteries need characterization.

Capacity estimation is important when determining factors such as SOH and SOC. An incorrect estimation can lead to skewed data for these important parameters. One issue that may occur is overall battery pack failure. In addition to this, it directly impacts performance, reliability, and longevity of the batteries life cycle. An accurate capacity estimation facilitates precise energy management, preventing premature battery depletion or overcharging, which can lead to safety hazards. Currently, a traditional approach to capacity estimation does not consider the voltage drop that occurs near the upper and lower bounds of charging. A full representation of the capacity may not be seen when tests are done this way.

In this thesis, an improved characterization algorithm using higher C-rate charging/discharging is presented. This algorithm reduces the time to characterize a battery to a fifth of the conventional characterization method. This will allow for high speed characterization while still keeping a low error in the different estimated parameters. Thus, the decision to reuse or recycle can be made much quicker and thus allows a more efficient cycle. Additionally, an improved capacity estimation algorithm including the factor of voltage drop in calculations is presented. This new addition will provide a more accurate representation of the capacity due to over-charging and over-discharging of the battery. Thus, more accurate parameter estimation can be made overall to ensure safety, and reliability.

## 1.1 Organization of the Thesis

The thesis is presented in the manuscript format with 4 Chapters. The remainder of the thesis is as followed: Chapter 2 details the Fast OCV characterization algorithm created to reduce the characterization time by five fold to obtain the OCV parameters. Chapter 3 details a comparison of a OCV offset approach to offset the voltage drop to balance OCV parameters between C-rates. Chapter 4 concludes the thesis.

## 1.2 Bibliography

- [1] G. S. Misyris, D. I. Doukas, T. A. Papadopoulos, D. P. Labridis, and V. G. Agelidis, “State-of-charge estimation for li-ion batteries: A more accurate hybrid approach,” *IEEE Transactions on Energy Conversion*, vol. 34, no. 1, pp. 109–119, 2018.

## Chapter 2

# A Fast OCV Characterization Approach for Battery Reuse Applications



## 2.1 Introduction

Li-ion batteries have been used in current-day electric vehicles (EVs). To provide safety, reliability, and efficiency for these batteries, the battery packs must be monitored. A Battery management system (BMS) monitors the current, temperature, and instantaneous voltage and also performs different control operations [1]. The BMS functions by performing corrective actions to ensure safety by estimating crucial parameters of the battery such as - battery impedance, State-of-charge (SOC), capacity, state-of-health (SOH), time to shut down, and the remaining useful life.

SOC estimation is an important parameter for the functioning of a BMS [2,3]. It is equivalent to a fuel gauge indicator in gasoline vehicles. The SOC of any battery gives the percentage of the remaining charge as a function of the total battery capacity. The SOC is computed usually through coulomb counting [4], voltage lookup method [5] or by use of a combined estimation approach [6]. For the voltage-based approach to SOC estimation, the OCV parameters are required. These parameters are calculated using curve-fitting functions representing the non-linear relationship. However, the OCV characterization test using slow and constant current takes approximately 60 hours.

Battery reuse is a common reoccurrence in today's batteries [7]. Current batteries in EVs outlive the life of the car itself [8]. From here, we are provided with two options: reuse the battery, or recycle the battery into components for future use [9]. Currently, a traditional OCV method is employed to evaluate battery degradation. This is a process which takes around 60 hours to completely characterize a battery. Characterizing reused batteries must be done case by case due to the differences in usage and environment the battery was used in.

Thus, it is evident that a new approach is needed to characterize a battery in short time. The objective of this thesis is to explore a new OCV characterization approach to reduce the time needed to characterize any battery. In summary, the contributions

are listed below:

1. In this thesis, we propose a data collection plan for OCV-SOC characterization that reduces the characterization time to 1/5 of the time it would take using a traditional approach.
2. A new approach is presented for the OCV-SOC characterization when the current is changing.

The proposed approach was tested on 4 batteries for consistency. Additional tests of SOC and OCV error modelling was done and an error of less than 3% was observed. The rest of the thesis is organized as follows: A review of the traditional OCV modelling approach is done in section 2.2. In section 2.3 we explore the current charging strategies in depth that are used within the experiment. We explain the slow traditional OCV method as well as our proposed fast charging method. Section 2.5 shows our experimental details, such as batteries, and testing equipment, as well as a data collection plan for both our methods. The results of our findings are presented in section 2.6. Section 2.7 concludes the thesis.

## 2.2 OCV Modeling Approaches

### 2.2.1 Traditional OCV modelling approach

In figure 3.16, the equivalent circuit model (ECM) of the battery used to derive the parameter estimation equations is shown.

From the ECM, the measured voltage across the battery terminals is

$$z_v[k] = v[k] + n_v[k] \tag{2.1}$$

where  $v[k]$  is the true voltage across the battery terminals and  $n_v[k]$  is the voltage

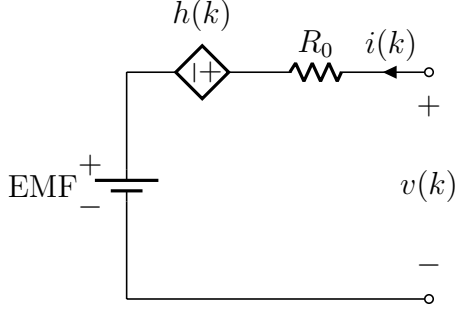


Figure 2.1: **DC equivalent circuit model.**

measurement noise which is modeled as white Gaussian. During the OCV experiment i.e., when the battery is being slowly charged/discharged, the terminal voltage  $z_v[k]$  can be written as

$$z_v[k] = V_o(s[k]) + h[k] + i[k]R_0 + n_v[k] \quad (2.2)$$

where  $h[k]$  is the hysteresis or voltage "pull" which is a function of current and SOC of the battery[\*ref\*]. Since the OCV test is performed at a very low current, it is assumed that the hysteresis is proportional to the current only and hence, the measurement can be written as

$$z_v[k] = V_o(s[k]) + i[k]R_{0,h} + n_v[k] \quad (2.3)$$

where the effective resistance is

$$R_{0,h} = R_0 + R_h \quad (2.4)$$

is the sum of the battery series resistance  $R_0$  and the constant current hysteresis equivalent resistance  $R_h$ . With this information, the parameter estimation for the models can be derived.

The SOC can be computed as

$$s[k] = s[k-1] + \frac{\Delta i[k]}{3600Q} \quad i = 1, \dots, N \quad (2.5)$$

where the initial SOC is  $s[0] = 1$ ,  $Q$  is the battery capacity, and  $\Delta$  is the sampling time. Considering that the OCV characterization requires the battery to be emptied and charged back, the final SOC value will be  $s[N] = 1$  as well.

Due to the numerical instability that may happen when SOC,  $s = 0$  and  $1$ , the linear scaling approach is applied to the system. The scaling approach allows us to map the SOC  $\in [0,1]$  to SOC  $\in [0+\epsilon,1-\epsilon]$ . Doing this, prevents  $s'$  from reaching  $0$  or  $1$ , thereby avoiding instability [10]. First, the new SOC will be scaled as

$$s' = (1 - 2\epsilon)s + \epsilon \quad (2.6)$$

where  $\epsilon$  is selected based on each model. It can be seen through [10] that  $\epsilon = 0.175$  gives the most optimal results in the Combined model as well as its variants. Due to this,  $\epsilon = 0.175$  will be utilized for the entirety of the tests.

### 2.2.1.1 Combined+3 Model

The Combined +3 model is a variation of the combined model. It allows for the capturing of the "sharp decline" [11] by additionally adding the 3 terms:  $1/s^2$ ,  $1/s^3$ , and  $1/s^4$ . The Combined+3 model parameters can therefore be derived as

$$V_0(s) = k_0 + k_1s + k_2s^{-2} + k_3s^{-3} + k_4s^{-4} \quad (2.7)$$

$$+k_5s + k_6\ln(s) + k_7\ln(1 - s)$$

Thus, 2.3 can then be written as

$$z_v[k] = V_o(s[k]) + i[k]R_{0,h} + n_v[k] \quad (2.8)$$

This is written in vector form as

$$z_v[k] = \underbrace{\begin{bmatrix} \mathbf{p}_o(s[k])^T & i[k] \end{bmatrix}}_{\mathbf{p}[k]^T} \underbrace{\begin{bmatrix} \mathbf{k}_o \\ R_{0,h} \end{bmatrix}}_{\mathbf{k}} + n_v[k] \quad (2.9)$$

where

$$\mathbf{k}_o = \begin{bmatrix} k_0 & k_1 & k_2 & k_3 & k_4 & k_5 & k_6 & k_7 \end{bmatrix} \quad (2.10)$$

and

$$p_o(s[k])^T = [1 \ \frac{1}{s[k]} \ \frac{1}{s^2[k]} \ \frac{1}{s^3[k]} \ \frac{1}{s^4[k]} \ s[k] \ \ln(s[k]) \ \ln(1-s[k])] \quad (2.11)$$

By considering a batch of  $N$  voltage measurements, equation 2.9 can be written in the form

$$\mathbf{v} = \mathbf{P}\mathbf{k} + \mathbf{n} \quad (2.12)$$

where

$$\mathbf{v} = \begin{bmatrix} z_v[1] & z_v[2] & \cdots & z_v[t_N] \end{bmatrix}^T \quad (11)$$

$$\mathbf{P} = \begin{bmatrix} p[1] & p[2] & \cdots & p[t_N] \end{bmatrix}^T \quad (12)$$

$$\mathbf{k} = \begin{bmatrix} k_0 & k_1 & k_2 & k_3 & k_4 & k_5 & k_6 & k_7 & R_{0,h} \end{bmatrix}^T \quad (13)$$

$$\mathbf{n} = \begin{bmatrix} n[1] & n[2] & \cdots & n[t_N] \end{bmatrix}^T \quad (14)$$

The least-square estimate of the parameter vector is given by

$$\mathbf{k} = (\mathbf{P}^T\mathbf{P})^{-1}\mathbf{P}^T\mathbf{v} \quad (2.15)$$

Now, for a given SOC, the corresponding estimate  $\hat{V}_o$  is computed as

$$V_o = \mathbf{p}_o(s)^T\mathbf{k}_o \quad (2.16)$$

## 2.2.2 OCV Modelling Through Averaging

In this section, a second approach to OCV-SOC modelling is presented. This approach is suitable to obtain OCV-SOC parameters without the current assumption made in Section 2.2.1.

For example, consider a current profile that is not slow and constant. Then the OCV modelling approach given in the previous section cannot be applied. Thus, in this thesis, an approach to estimate the OCV of the battery using the terminal voltage is proposed when the current assumption fails. For the equivalent circuit model in Figure 3.16, the estimate of the resistance is used to calculate the voltage drop across the resistor  $i(k) \times \hat{R}_0$ . Using this, an estimate of OCV is obtained as

$$\hat{V}_o(k) = v(k) - i(k)\hat{R}_0 \quad k = 1, \dots, N \quad (2.17)$$

The estimate of OCV in (2.17) suffers from hysteresis and relaxation effects, especially if the current  $i(k)$  changes during the experiment.

The corresponding SOC values  $s[k]$  (see (2.5)) are now divided into  $T_b$  bins. Table 2.1 shows the SOC values and the corresponding OCV for each bin. The  $i^{\text{th}}$  values in the bin is computed as follows:

$$\bar{V}_o(i) = \frac{1}{L} \sum_{l=1}^L \hat{V}_o(l) \quad i = 1, \dots, L_b \quad (2.18)$$

$$\text{s.t. } (i-1)/L_b < s(l) < i/L_b \quad (2.19)$$

Figure 2.2 shows the computed  $\hat{V}_o(k)$  values (blue) and the averaged  $\bar{V}_o(i)$  values (red) for data collected from a sample battery.

Now, the vector observation model (2.12) can be rewritten as

$$\mathbf{v} = \mathbf{P}\mathbf{k} + \mathbf{n} \quad (2.20)$$

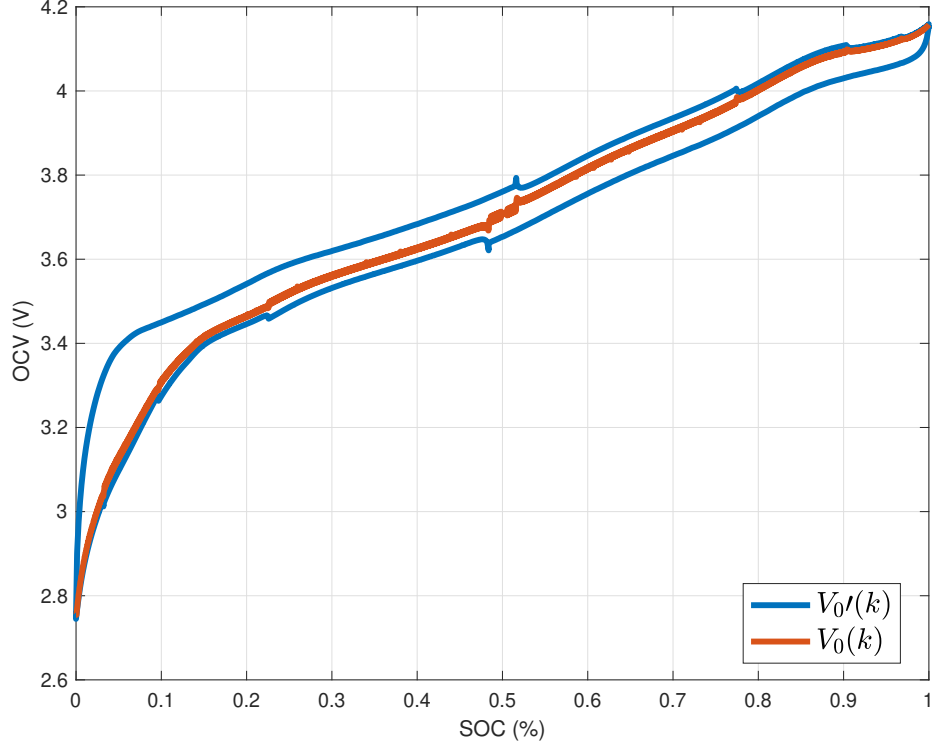


Figure 2.2: An estimate of OCV is calculated by averaging  $\hat{V}_o'(k)$  over a window of the length  $T_w$ .

Table 2.1: Pairs of OCV-SOC values

Bin number	1	2	...	$i$	...	$L_b$
SOC	$1/L_b$	$2/L_b$		$i/L_b$		1
OCV	$V_o(1)$	$V_o(2)$		$V_o(i)$		$V_o(L_b)$

where

$$\mathbf{v} = [\bar{V}_o(1) \quad \bar{V}_o(2) \quad \dots \quad \bar{V}_o(L_b)]^T \quad (2.21)$$

$$\mathbf{P} = [\mathbf{p}_o(\bar{s}[1]) \quad \mathbf{p}_o(\bar{s}[2]) \quad \dots \quad \mathbf{p}_o(\bar{s}[L_b])]^T \quad (2.22)$$

$$\mathbf{k} = [k_0 \quad k_1 \quad k_2 \quad k_3 \quad k_4 \quad k_5 \quad k_6 \quad k_7]^T \quad (2.23)$$

$$\mathbf{n} = [n[1] \quad n[2] \quad \dots \quad n[L_b]]^T \quad (14)$$

and

$$\bar{s}[i] = \frac{i}{L_b}, \quad i = 1, \dots, L_b \quad (2.24)$$

Now, the OCV parameters can be estimated through least squares similar to (2.15).

## 2.3 Charging Strategies for OCV test

Common charging strategies include different constant-current methods [12]. Present OCV-SOC modelling requires C/30 discharge and then C/30 Charge described in Section 2.3.1. The corresponding OCV estimation is found in Section 2.2.1. Another is the multi-step constant-current method (MCC) which involves multiple step drops of current every hour. The proposed approach consists of this changing current as seen in Section 2.3.1 and 2.3.2. These methods are discussed and experimented on.

### 2.3.1 Characterization approach (Slow Method)

A constant current-constant voltage (CC-CV) charging strategy is followed to fully charge the battery before conducting an OCV-SOC test. A low current slow discharge charge of the battery is pursued to perform the OCV-SOC test.

1. A constant current is supplied to the battery until the terminal voltage reaches 4.2V.
2. The terminal voltage is maintained at 4.2V for constant voltage charging until the current drops to 0.005A
3. The battery is rested for one hour.
4. A constant current of C/30 is supplied to slowly discharge the battery for thirty hours until the SOC reaches 0%. A rest of 1 hour follows, before the battery is charged back again by C/30 for thirty hours until the SOC reaches 100%



### 2.3.2 Characterization approach (Fast Method)

The solution to reducing the characterization time is a change in the current profile to charge and discharge the battery. This is done by charging the battery at a higher current in order to reduce the time. The approach we will take is a multi-step constant current (MCC) approach. Starting by discharging at a high C rate and dividing by a fraction every hour. A detailed collection plan is shown in figure 2.3. This solution will allow for a characterization time of 11 hours and greatly reduce the time needed to characterize any battery.

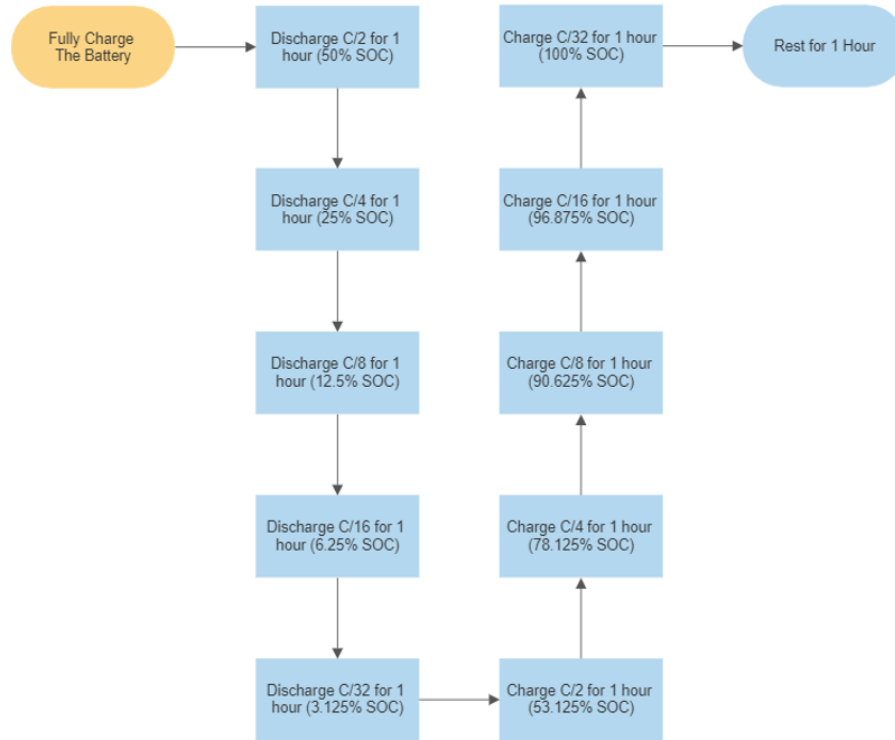


Figure 2.3: **Fast Charge collection plan tested during the experiment as well as the expected SOC after each step**

A constant current-constant voltage (CC-CV) charging strategy is followed to fully charge the battery before conducting an OCV-SOC test. A multistep-constant current (MCC) charging strategy then follows to discharge and charge the battery to perform the OCV-SOC test. A data collection plan can visual can be referred to in Figure 2.3.

1. A constant current is supplied to the battery until the terminal voltage reaches 4.2V.
2. The terminal voltage is maintained at 4.2V for constant voltage charging until the current drops to 0.005A
3. The battery is rested for one hour.
4. A constant current of  $C/2$  is supplied to discharge the battery for 1 hour, then  $C/4$  for 1 hour, then  $C/8$ ,  $C/16$ , and finally  $C/32$  for an hour.
5. After the battery is fully discharged, this process similarly continues for the charging process, where the battery is charged at  $C/2$  for 1 hour, then  $C/4$ , then  $C/8$ ,  $C/16$ , and finally  $C/32$  for an hour.
6. The battery is then finally rested for one hour.

## 2.4 Performance metrics

To evaluate the error in SOC and OCV estimation in the proposed fast OCV-SOC characterization method and to compare its accuracy with the traditional OCV approach, two error metrics are defined. The error in SOC  $s[k]$  is defined as the percentage of difference in SOC estimated between the fast  $s[k]$  and slow  $s'[k]$  characterization method.

$$\text{Error}(s[k]) = 100 \times (s[k] - s'[k])^2 \quad \forall k = 1, 2, 3, \dots, N \quad (2.25)$$

The error in OCV  $s[k]$  is defined as the percentage of difference in OCV estimated between the fast  $V_0[k]$  and slow  $V'_0[k]$  characterization method.

$$\text{Error}(V_0[k]) = 100 \times (V_0[k] - V'_0[k])^2 \quad \forall k = 1, 2, 3, \dots, N \quad (2.26)$$

## 2.5 Experimental Details

The experiment was done using 4 LG 18650 batteries with a 3.4Ah capacity using the characterization techniques described previously in Section 2.3. The data collection is performed using an Arbin BT-2000 battery cycler shown in Figure 2.4. It has 16 independently controlled channels, each with a voltage range of 0-5V and a current range of  $\pm 10\text{A}$ . Four of these channels are used simultaneously to collect OCV-SOC data such as current and voltage from all four cells at room temperature. A current profile, shown in Figure 2.6(top) is applied to the battery and the voltage across the battery terminals shown in Figure 2.6(bottom) is recorded.

To employ both the slow and fast approaches, the traditional OCV method is followed by the proposed plan for fast characterization. The voltages, current, and time data are recorded for both approaches. The traditional OCV test took approximately 70 hours and the proposed Fast OCV test took 11 hours. Furthermore, the SOC and OCV error metrics in Section 2.4 are calculated.

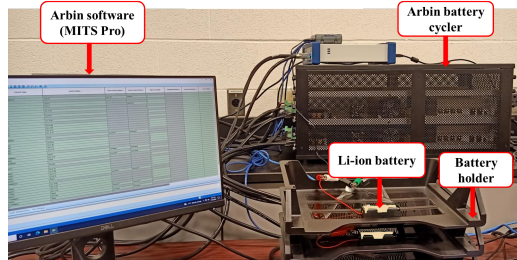


Figure 2.4: Experimental setup for battery testing [13]

## 2.6 Results

The voltage and current data recorded using the Arbin BT-2000 battery cycler is used to obtain a typical OCV-SOC curve represented by the Combined+3 model. The OCV characterization is done using three approaches:

1. Slow OCV characterization using the traditional OCV modelling approach (Slow).

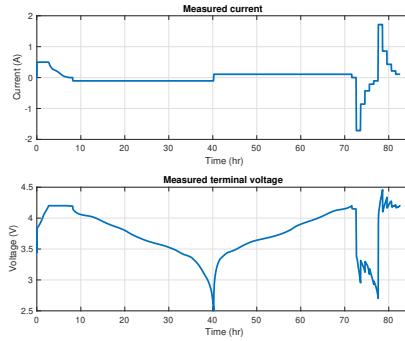


Figure 2.5: The current profile recorded for all four batteries is shown here. The traditional OCV test is followed by the fast OCV characterization test.

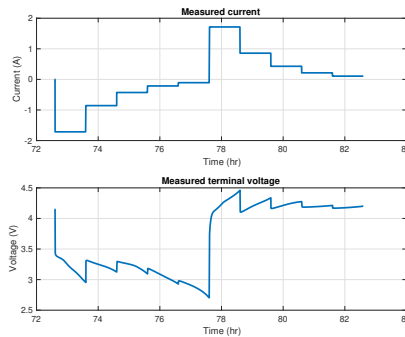


Figure 2.6: The current profile recorded for the fast characterization method is shown here.

2. Fast OCV characterization using the traditional OCV modelling approach (Fast OCV - I).
3. Fast OCV characterization using the OCV modelling through the averaging approach (Fast OCV - II).

Figure 2.7 shows the plots of the OCV-SOC curve found using the Combined +3 model for all three methods. It can be seen that the three methods are comparable in the OCV-SOC characterization and that the proposed approach has the capability of characterizing the OCV-SOC relationship faster than the traditional OCV approach.

Table 2.2 is a comparison between the capacities of the slow method against the fast method. A small difference in capacity can be seen between the Slow vs Fast where we see a decrease in capacity in the fast charging method. This is subject to

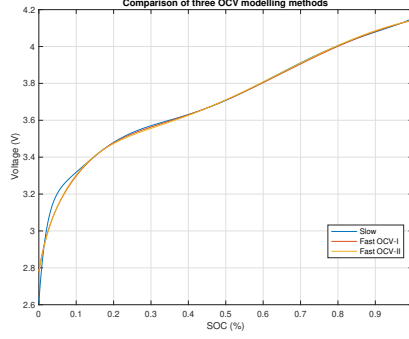


Figure 2.7: OCV-SOC curves estimated for all four batteries using the Combined+3 model.

happen due to the differences in prior charging methods compared to that during the experiment

Table 2.2: Capacities of both charging methods Slow vs. Fast

Cell	Slow Approach (C/32)	Fast MCC Approach
Cell 1	3.3860	3.3207
Cell 2	3.3847	3.3142
Cell 3	3.3421	3.3067
Cell 4	3.3870	3.3028

Shown in Table 2.3 is the internal resistance of all 4 cells at all points of SOC. We see very small differences near the low SOC regions. This internal resistance is calculated utilizing the change in current as well as the change in voltage that occurs 5 times during charge and discharge. From here we can calculate the internal resistance of the battery.

Figure 2.8 shows the OCV error calculated using (2.25) for Method 2 of OCV characterization. This error is calculated as the difference in voltage with the traditional slow OCV characterization. It can be seen that the error is at its highest during the low SOC regions and only minimal error is observed at higher SOC regions. This shows the benefits of the Fast method in terms of voltage error. In Figure 2.8, the SOC error for each battery cell is shown for Method 2. Using (2.26), the SOC error is calculated as the difference between the SOC estimated using traditional slow and fast

Table 2.3: Internal resistances of all 4 cells at different SOC's

SOC (%)	Cell - 1	Cell - 2	Cell - 3	Cell - 4
99.99	0.3951	0.4088	0.3990	0.3554
48.38	0.3993	0.4066	0.4114	0.3575
22.58	0.3891	0.3972	0.4027	0.3490
9.67	0.3975	0.4061	0.4105	0.3568
3.22	0.4233	0.4349	0.4369	0.3831
0	0.3936	0.4014	0.4061	0.3514
0	0.4408	0.4487	0.4514	0.3931
51.61	0.3991	0.4060	0.4113	0.3578
77.42	0.3888	0.3963	0.3988	0.3492
90.32	0.3870	0.3952	0.3977	0.3483
96.77	0.3887	0.3977	0.3994	0.3505

OCV characterization methods. The errors found in Figure 2.8, are also translated into the SOC error in this figure. It can be observed that the Fast OCV modelling approach has a maximum SOC error in the lower SOC regions of approximately 2%.

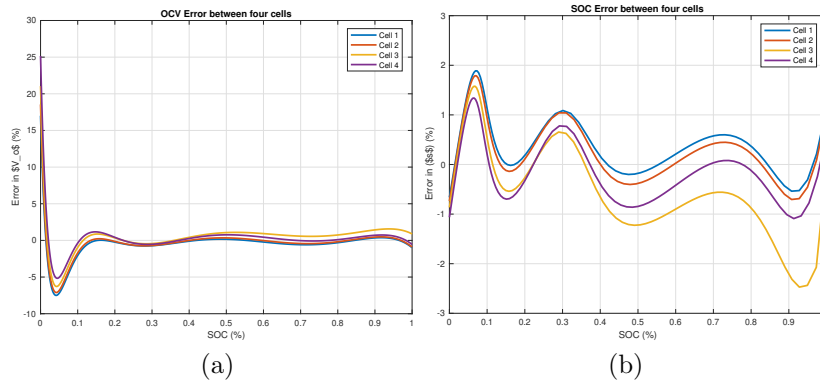


Figure 2.8: OCV error obtained through the difference in voltages between the true voltage (slow method) compared to the fast OCV characterization using the traditional OCV modelling approach (Fast OCV - I).

Similarly, Figures 2.9 show the OCV and SOC estimation error for Method 3 of Fast OCV characterization. Higher errors in OCV estimation again were found at lower SOC values. The approximation of voltage drop using the OCV averaging approach also resulted in a SOC error of approximately 2.2%. Thus, these results show

that our fast OCV characterization approach successfully characterized the battery faster than a traditional approach while keeping minimal error and providing similar results. Future improvements are explored in the conclusion on methods to create a more optimized current profile to possibly speed up the time to characterize even further.

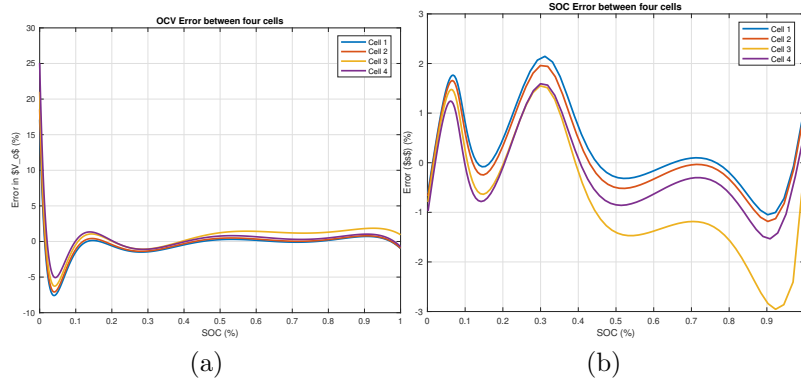


Figure 2.9: OCV error obtained through the difference in voltages between the true voltage (slow method) compared to the Fast OCV characterization using the OCV modelling through the averaging approach (Fast OCV - II).

## 2.7 Conclusions

This thesis presents a new Fast charge OCV characterization approach for the characterization of batteries with an emphasis on reducing the time to characterize a battery through a multi-step constant current approach. Differences in capacities and differences in characterization are seen and analyzed. The proposed approach was tested on 4 batteries and it was found to be consistent. Overall, it is seen that the proposed approach provides an accurate and reliable characterization of the battery at a fraction of the time of the compared approach.

Some works that are being looked at and experimented on currently are starting the current profile at a higher current. This will allow for a faster charge overall and will reduce the time of characterizing greatly. Another would be to experiment

with different current profiles such as C/32, C/64, or even C/128 to change the results or provide results different from the current expectations. Right now, our experiment ends with C/32 for 1 hour. Will adding a C/64 and C/128 cycle prove to be more effective in characterizing the battery or is up to C/32 enough for the application? These works can allow for a more rounded and optimized approach and will be explored in the future.

## 2.8 Bibliography

- [1] G. S. Misyris, D. I. Doukas, T. A. Papadopoulos, D. P. Labridis, and V. G. Agelidis, “State-of-charge estimation for li-ion batteries: A more accurate hybrid approach,” *IEEE Transactions on Energy Conversion*, vol. 34, no. 1, pp. 109–119, 2018.
- [2] G. Dong, Y. Xu, and Z. Wei, “A Hierarchical Approach for Finite-Time H- $\infty$  State-of-Charge Observer and Probabilistic Lifetime Prediction of Lithium-Ion Batteries,” *IEEE Transactions on Energy Conversion*, vol. 37, no. 1, pp. 718–728, 2022.
- [3] K. Yu, H. Wang, L. Mao, Q. He, and Q. Wu, “Ic curve-based lithium-ion battery soc estimation at high rate charging current,” *IEEE Transactions on Instrumentation and Measurement*, vol. 71, pp. 1–9, 2022.
- [4] K. Movassagh, A. Raihan, B. Balasingam, and K. Pattipati, “A critical look at coulomb counting approach for state of charge estimation in batteries,” *Energies*, vol. 14, no. 14, 2021.
- [5] M. Petzl and M. A. Danzer, “Advancements in OCV measurement and analysis for lithium-ion batteries,” *IEEE Transactions on Energy Conversion*, vol. 28, no. 3, pp. 675–681, 2013.



- [6] H. Movahedi, N. Tian, H. Fang, and R. Rajamani, “Hysteresis compensation and nonlinear observer design for state-of-charge estimation using a nonlinear double-capacitor li-ion battery model,” *IEEE/ASME Transactions on Mechatronics*, 2021.
- [7] E. Martinez-Laserna, E. Sarasketa-Zabala, I. V. Sarria, D.-I. Stroe, M. Swierczynski, A. Warnecke, J.-M. Timmermans, S. Goutam, N. Omar, and P. Rodriguez, “Technical viability of battery second life: A study from the ageing perspective,” *IEEE Transactions on Industry Applications*, vol. 54, no. 3, pp. 2703–2713, 2018.
- [8] E. Braco, I. San Martín, A. Berrueta, P. Sanchis, and A. Ursúa, “Experimental assessment of first-and second-life electric vehicle batteries: Performance, capacity dispersion, and aging,” *IEEE Transactions on Industry Applications*, vol. 57, no. 4, pp. 4107–4117, 2021.
- [9] E. Hossain, D. Murtaugh, J. Mody, H. M. R. Faruque, M. S. H. Sunny, and N. Mohammad, “A comprehensive review on second-life batteries: Current state, manufacturing considerations, applications, impacts, barriers & potential solutions, business strategies, and policies,” *Ieee Access*, vol. 7, pp. 73215–73252, 2019.
- [10] M. S. Ahmed, S. A. Raihan, and B. Balasingam, “A scaling approach for improved state of charge representation in rechargeable batteries,” *Applied energy*, vol. 267, p. 114880, 2020.
- [11] B. Pattipati, B. Balasingam, G. Avvari, K. Pattipati, and Y. Bar-Shalom, “Open circuit voltage characterization of lithium-ion batteries,” *Journal of Power Sources*, vol. 269, pp. 317–333, 2014.

- [12] J. Jiang, Q. Liu, C. Zhang, and W. Zhang, "Evaluation of acceptable charging current of power li-ion batteries based on polarization characteristics," *IEEE Transactions on Industrial Electronics*, vol. 61, no. 12, pp. 6844–6851, 2014.
- [13] P. Kumar, G. Rankin, K. R. Pattipati, and B. Balasingam, "Model-based approach to long term prediction of battery surface temperature," *IEEE Journal of Emerging and Selected Topics in Industrial Electronics*, vol. 4, no. 1, pp. 389–399, 2022.

## Chapter 3

### Offsetting Approach for Capacity

### Estimation in Li-ion Batteries

### 3.1 Introduction

The global shift from gasoline-powered vehicles to electric vehicles has sparked increased attention toward Li-ion batteries. Li-ion batteries have been consistently used in the past 30 years in wide-ranging portable applications that require high energy capacity [1]. A big application is in electric vehicles (EVs). Lithium-ion batteries have become an important component within EVs, serving as the primary power source. Multiple battery cells are organized in series, parallel, or hybrid series-parallel arrangements to fulfill the specifications for voltage and power demands. For monitoring of these packs, electric vehicles are equipped with a battery management system (BMS) [2]. The BMS functions by performing corrective actions to ensure safety by estimating crucial parameters of the battery such as - battery impedance, State-of-charge (SOC), capacity, state-of-health (SOH), time to shut down, and the remaining useful life.

State of Charge (SOC) estimation stands as a critical factor influencing the operation of a Battery Management System (BMS) [3,4]. Comparable to a fuel gauge in conventional gasoline vehicles, SOC represents the remaining charge as a percentage of total battery capacity. SOC is typically determined through techniques such as coulomb counting [5], voltage lookup methods [6], or a hybrid estimation approach [7]. This characterization is done using multiple methods and allows for a wide range of time taken and accuracy of data.

The characterization of OCV-SOC relationship varies in standardization when applied in industrial settings, typically conducted using a representative battery sample. Subsequently, the OCV-SOC characterization data is compiled into a table format for utilization across various battery cells or packs. Usually, the characterization techniques are divided into two main categories: Galvanostatic Intermittent Titration Technique (GITT) and the low-rate cycling method [8]. The GITT technique involves discharging the sample battery in increments of 10% across the entire SOC

range. During each of these steps, a brief 10-second charge/discharge pulse is applied to obtain the estimation of additional battery parameters. The low-rate cycling approach involves fully discharging a full sample battery until depletion, followed by recharging it to maximum capacity. During this process, voltage and current data are collected and subsequently subjected to curve-fitting methods to characterize the OCV relationship. Unlike the standardized GITT technique, the low-rate cycling method lacks standardization, and the literature does not define a specific current rate for conducting this test. Additionally, these current rates create an error in capacity due to the low-rate cyclers stopping prematurely at set voltages.

The cycle rate creates a uncertainty in the capacity due to the cycling process of a set battery. The inaccuracies that result from the cycling process can be attributed to internal resistance of the battery as well as the cycle rate. Currently, battery charging algorithms are not accounting for the increase in voltage due to the internal resistance which in turn, causes an inaccuracy in the calculated charge and discharge capacity of the battery. This thesis emphasizes a focus on neutralizing that inaccuracy in the capacity by offsetting the battery voltage parameters by a predetermined amount of voltage.

The remainder of this paper is organized as follows: Section 3.2 present the voltage difference approach and ideology behind the approach. Section 3.3 presents an explanation in the proposed charging algorithm utilized in the paper. Section 3.4 presents a detailed representation of the algorithm used and the detailed approach. Section 3.5 presents the values used to perform the new algorithm created based on previous experiments. Section 3.6 presents the details of the (identical) batteries used for the analysis and the details of the scientific grade high-precision data collection system. Section 3.7 clearly defines the capacity comparison metrics to be computed based on the collected data. Section 3.8 presents the capacity comparison metrics, defined in Section 3.7. Finally, the paper is concluded in Section 3.9.

## 3.2 Voltage Difference

Voltage difference can be described as the voltage drop seen when charging/discharging a battery near its  $OCV_{max}$  and  $OCV_{min}$ , where  $OCV_{max}$  is the high voltage limit of the selected battery and  $OCV_{min}$  is the low voltage limit. This causes the voltage limits set to be reached at a much earlier time, which leads to a non full charge/discharge cycle. This voltage will change based on charge rate as well as the internal resistance of the battery, thus the voltage drop value will vary between batteries. The value of voltage difference can be defined through the formula

$$v_d = IR_0 \quad (3.27)$$

where  $I$  is the charge/discharge current and  $R_{0h}$  is the internal resistance of the given battery.

## 3.3 Battery Cycling

The planned experiment involves utilizing constant-current(CC) charging and discharging. The battery is charged and discharged at multiple c-rates to check for accuracy. The algorithm 1 involves a constant current constant voltage charge until  $OCV_{max}$  plus the calculated voltage difference. This will ensure an overcharge so that we can account for the voltage difference stated in 3.5. After this, an over discharge constant current of C/N is applied until the battery reaches  $OCV_{min}$  minus the voltage difference. Finally, the battery is once again overcharged back to  $OCV_{max}$  plus the calculated voltage difference. This test ensures that the battery capacity can be observed and compared to previous results. The collected data is parsed offline and findings are observed.

### 3.4 Low-Rate-OCV-Test (N)

In this section, the detailed approach to performing the low-rate open circuit voltage test is presented. Utilizing previous information, we are able to compensate by resetting the  $OCV_{min}$  and  $OCV_{max}$  by the calculated voltage difference. Here, the input N refers to C/N the constant charging current used to perform the test. The algorithm 1 describes the Low-Rate-OCV testing.

---

**Algorithm 1** Low-Rate-OCV-Test ( $N, T$ )

---

- 1: Set Temperature:  $T$
  - 2: CC-CV-Charge( $C/N, OCV_{max} + V_d, 1C$ )
  - 3: 1-hour Rest
  - 4: **while**  $v > OCV_{min} - V_d$  **do**
  - 5:     CC-discharge ( $C/N$ )  
      Sample data at 1/60 Hz
  - 6: **end while**
  - 7: **while**  $v < OCV_{max} + V_d$  **do**
  - 8:     CC-charge ( $C/N$ )  
      Sample data at 1/60 Hz
  - 9: **end while**
  - 10: 1-hour Rest
  - 11: **Discharge Internal Resistance Test**
- 

### 3.5 Value of $V_d$ at different OCV rates

In [9], the voltage difference was calculated at each C-rate 4 times with unique batteries. In this section we discuss the averaging of the value of  $V_d$  by averaging the 4 cells at each rate. The values are shown in Table 3.5.

### 3.6 Experimental Details

This section outlines the configuration for data collection and the batteries employed to gather low-rate OCV test data within a controlled laboratory environment.

### 3.6.1 Data Collection System

The voltage and current data from the battery were collected using a scientific-grade battery cycler made by Arbin Inc. The MITS Pro is Arbin's comprehensive battery testing software that allows programming each channel to a specific data collection plan. Figure 3.10 shows a picture of the Arbin laboratory battery testing (LBT) system which can be used to cycle 16 batteries simultaneously at a given time. Figure 3.10 shows a block diagram of the data collection system.

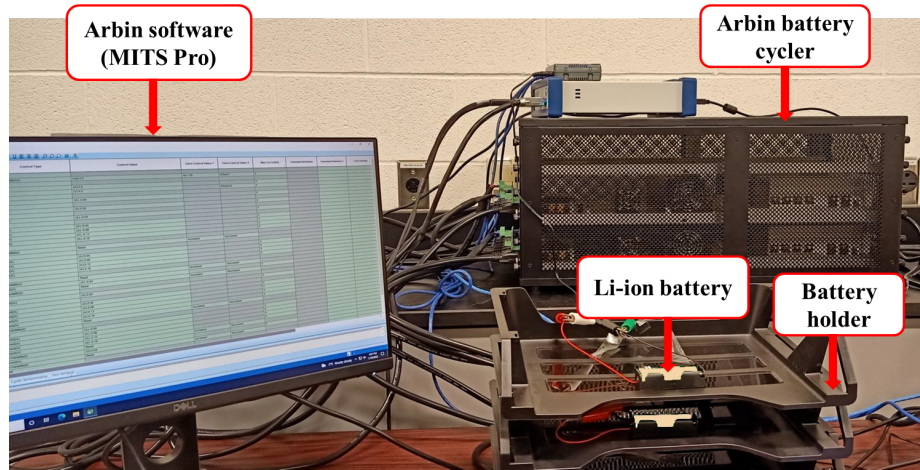


Figure 3.10: Arbin battery cycler.

Table 3.4:  $V_d$  at different OCV rates

OCV rate	Value of $V_d$ (mV)
$C/2$	73.42 V
$C/4$	51.30 V
$C/8$	37.63 V
$C/16$	31.57 V
$C/32$	26.07 V
$C/64$	23.23 V
$C/128$	21.93 V



### 3.6.2 Batteries

The data for the demonstration was based on Molicel INR-21700-P42A battery cells [10]. In total, 28 identical cells of the above serial number were used in the present study; these cells are labelled E3201, E3202, . . . , and E3228 using a permanent marker. Figure 3.11 shows a picture of five cells in the experiment. Each battery cell possesses a nominal voltage of 3.6V, accompanied by a typical capacity of 4 Ah and an internal resistance of approximately 16 m $\Omega$ . Table 3.5 summarises important features of the battery cell from the data sheet [10].



Figure 3.11: Molicel INR-21700-P42A batteries.

Table 3.5: Specifications of Li-ion battery.

Specification	Value
Nominal voltage	3.6V
Typical capacity	4000 mAh
Discharge current	45A
Height	70.2 mm
Diameter	21.7 mm
Weight	70g
Internal resistance	16 m $\Omega$

Table 3.6 summarizes the entire data collection plan carried out in this work. In summary, four batteries were selected and the OCV characterization data was collected from them according to the data collection plan described by the routine

‘Low-Rate-OCV-Offset’. The details and rationale of the low-rate OCV characterization data collection routine can be found in 1; in short, the details of

- (a) charging the battery before the experiment: the battery was first charged using a CC-CV approach with  $C/N$  as the shutdown current.
- (b) Then, the low-rate OCV test was carried out using a  $C/N$  current.
- (c) Finally, a current pulse series was applied to estimate the resistance.

are presented in 1. The data collection was repeated for seven different current rates ( $C/2$  to  $C/128$ ) at room temperature as shown in Table 3.6. Performance evaluation at different temperatures is deferred for future work.

Table 3.6: List of complete data collection

<b>Test</b>	<b>Battery numbers</b>
Low-Rate-OCV-Offset ( $C/2$ ,Room)	E3201, E3202, E3203, E3204
Low-Rate-OCV-Offset ( $C/4$ ,Room)	E3225, E3226, E3227, E3228
Low-Rate-OCV-Offset ( $C/8$ ,Room)	E3221, E3222, E3223, E3224
Low-Rate-OCV-Offset ( $C/16$ ,Room)	E3217, E3218, E3219, E3220
Low-Rate-OCV-Offset ( $C/32$ ,Room)	E3213, E3214, E3215, E3216
Low-Rate-OCV-Offset ( $C/64$ ,Room)	E3209, E3210, E3211, E3212
Low-Rate-OCV-Offset ( $C/128$ ,Room)	E3205, E3206, E3207, E3208

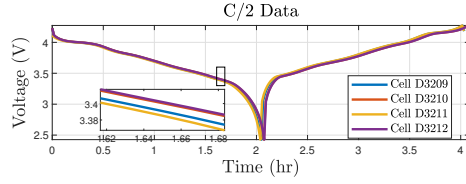
### 3.6.3 Voltage-Current Data

Figure 3.12 shows the voltage and current data for two different experiments (at  $C/2$  rate and  $C/128$  rate) listed in Table 3.6. Figure 3.12(a) and Figure 3.12(b) show the voltage and current data, respectively, collected during the low-rate OCV test at  $C/2$  rate (i.e, using the data collection algorithm Low-Rate-OCV-Test( $C/2$ ,Room)). Similarly, Figure 3.12(c) and Figure 3.12(d) show the voltage and current data, respectively, collected using the data collection algorithm Low-Rate-OCV-Test ( $C/128$ ,

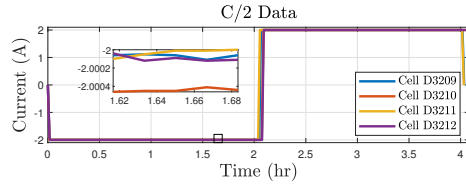
Room). A zoomed version of the curve shows the variations among the different C-Rates. It can be noticed from the zoomed portion that while the data collected at C/128 (from four different battery cells) overlays without many visible deviations, the data collected at the C/2 rate shows visible deviations. The goal of this thesis is to quantify the effect of such differences on the ultimate performance of the BMS, particularly in SOC estimation. Additionally, figure 3.13 shows a comparison of the terminal voltage of the offset and low-rate method. From here, we are able to clearly see that in the offset voltage, the terminal voltage reaches higher values at maximum when discharging as well as charging.

### 3.6.4 Analyzing the OCV curve

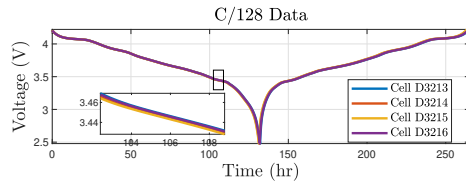
To begin the experiment, some assumptions were made with regards to the overcharge and over discharge process of the battery. From Figure 3.14, we can see that most of the batteries OCV and capacity comes from 10% SOC and on wards. We see that as the battery is between 10% and 0% SOC the batteries voltage starts to become volatile and rapid changes in OCV are seen. Due to this, we believed that we would be able to obtain accurate data when overcharging compared to over discharging. From figure 3.15, we can see the effect of the low-rate-OCV charging method. We can see that when charging to a normal 4.2V the SOC reached is only about 96% of the full SOC of the battery due to the voltage drop of the low-rate-OCV charging method. Overcharging by the value  $V_d$  allows for a full range of SOC when modeled and allows for a highly accurate representation of the batteries voltage and SOC.  $S_d$  is represented by the soc difference when overcharging vs the conventional charging method. When examining the low SOC regions, we can clearly see that overdischarging impacts a minute portion of the SOC, thus no clear examinations can be made at that volatile SOC region. In this test, we expect to obtain accurate data pertaining to the capacity while overcharging, while the over discharging data may be uncertain. This hypothesis is proven to be correct later on in this thesis, where the capacity gain



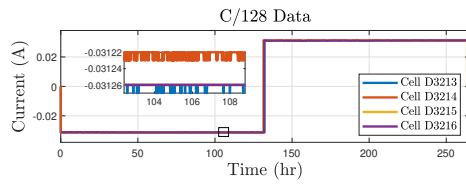
(a) Terminal voltage during the C/2 data collection.



(b) Current during the C/2 data collection.

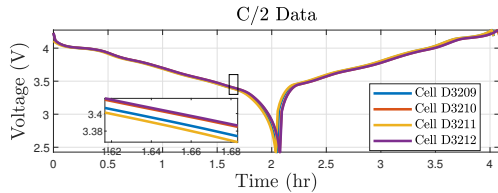


(c) Terminal voltage during the C/128 data collection.

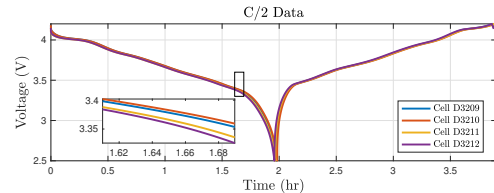


(d) Current during the C/128 data collection.

Figure 3.12: Low-rate OCV characterization data collected at the C/2 and C/128 rate.



(a) Terminal Voltage for Offset Method



(b) Terminal Voltage for Low-Rate-OCV Method

Figure 3.13: Terminal Voltage Comparison

is analyzed.

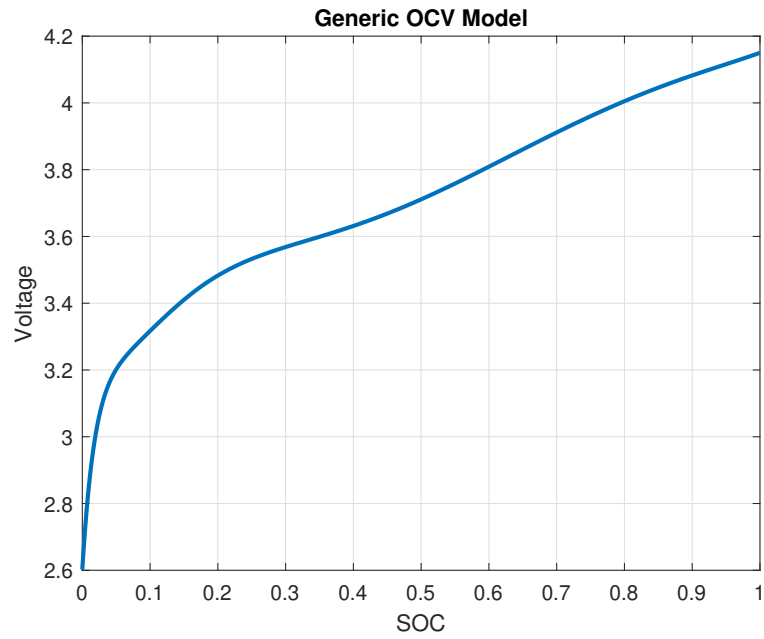


Figure 3.14: Generic OCV model

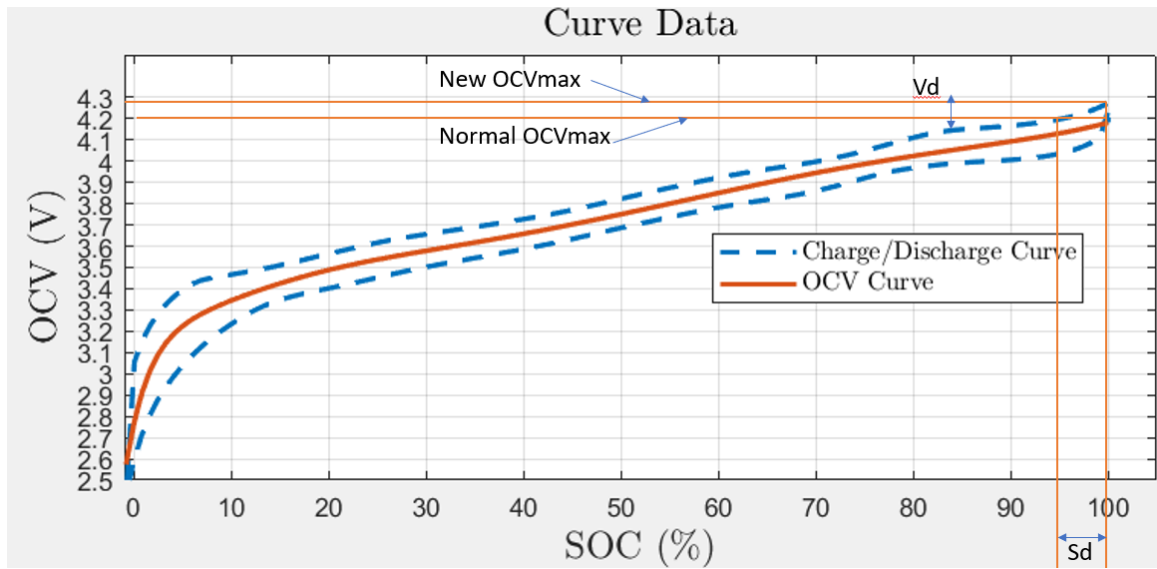


Figure 3.15: Charge/Discharge and Average OCV curve

### 3.6.5 Battery Voltage Drop

The main idea behind a overcharge and over discharge is to overcome the voltage drop that is seen due to the internal resistance of each battery. Each battery has a different internal resistance so this drop can be higher or lower determined by the capacity as well as the constant current charging rate. This voltage drop can be calculated as  $v_d = I_c R_{0h}$  during charging and  $v_d = I_d R_{0h}$  during discharging. From figure 3.16, we can see the relationship of the voltage drop through a DC equivalent circuit model, where  $R_{0h}$  represents the internal resistance and  $i(k)$  represents the charge/discharge rate.

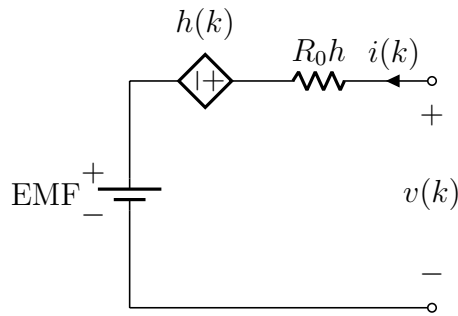


Figure 3.16: DC equivalent circuit model.

## 3.7 Computation of Comparison Metrics

In this section, the computations of the capacity comparisons at different C-rates is explained. Here, the data collected will be compared with previous literature [9] to understand the differences in capacity while using a voltage offset during the experiment process.

### 3.7.1 Computing the Battery Capacity

According to the OCV characterization data (shown for a  $C/2$  experiment in Figure 3.12 the battery was full ( $s = 1$ ) at the start of the experiment; and it was empty ( $s = 0$ ) at the end of discharge. Initially, this could only be an approximation due to the fact that there is a voltage drop at the amount of  $v_d = I_c R_{0h}$  during charging and  $v_d = I_d R_{0h}$  during discharging. But after the offset is accounted for in the charging algorithm, the capacity can be calculated due to the battery OCV reaching  $OCV_{\max}$  and  $OCV_{\min}$  during the charge/discharge process. This process counteracts the internal resistance of the battery and allows for an accurate representation of the capacity.

Thus, the capacity of the battery during discharging, denoted as  $Q_d$  and charging, denoted as  $Q_c$  can be defined as

$$Q_c = I_c t_c \quad \text{and} \quad Q_d = -I_d t_d \quad (3.28)$$

where  $I_c$  and  $I_d$  are the charge and discharge currents respectively, and  $t_c$  and  $t_d$  are the charge and discharge times respectively.

An average of these computed charge and discharge capacities can be defined as  $Q_{cavg}$  and  $Q_{davg}$  which is the average of the charge and discharge capacities at each C-rate. Similarly, the capacity of the offset test can similarly be defined as

$$Q_{co} = I_{co} t_{co} \quad \text{and} \quad Q_{do} = -I_{do} t_{do} \quad (3.29)$$

where  $I_{co}$  and  $I_{do}$  are the charge and discharge currents respectively during the offset experiment, and  $t_{co}$  and  $t_{do}$  are the charge and discharge times respectively during the offset experiment.

An average of these computed charge and discharge capacities can be defined as  $Q_{coavg}$  and  $Q_{doavg}$  which is the average of the charge and discharge capacities at each

## 3.8 Results

Shown in Figure 3.17 and 3.18, are the charge and discharge capacities comparisons of every battery at all C-rates tested with a voltage offset. From the figures, we see that our hypothesis that the lower the c-rate the higher the capacity due to the internal resistance of the battery. From figure 3.17, we see a considerable gain in capacity at all C-rates. This supports our idea of an increased capacity due to a voltage offset. Table 3.7 denotes individual charge and discharge capacities for non offset tests as well as with a voltage offset. From here we can see a similar pattern in which the charge capacity is greater than the discharge capacity for both methods.

From the average charge and discharge graphs and tables shown in Figure 3.19 and Table 3.8. We notice a increase in charge capacity going from non offset to offset. This further proves that capacity calculations are loss due to the internal resistance of the battery. Additionally, a clear outlier in the C/2 batteries can be seen in Figure 3.19. This can be due to the high effects of hysteresis at the highest charging rate. This causes the voltage to jump and leads to an inaccuracy as seen through the C/2 section in the figure. Apart from this c-rate, the other charging rates stay consistent with the hypothesis stated and allows for a further understanding of the effects of overcharging and overdischarging. Through overcharging, we are able to see a more accurate representation of the capacity of the battery due to the voltage drop that is seen while charging. For the discharge capacity, we are able to see an increase in capacity in the high C-rate charging experiments.

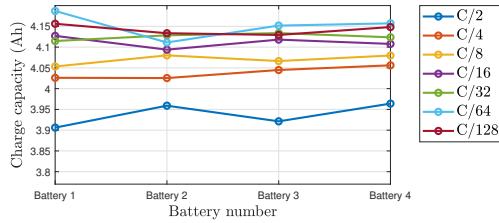


Table 3.7: Battery capacity estimates calculated at different C-Rates

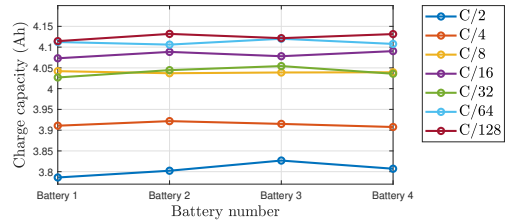
C-Rate	$i$ (A)	$Q_c$ (Ah)	$Q_d$ (Ah)	$Q_{co}$ (Ah)	$Q_{do}$ (Ah)
C/2	2	3.7860	3.9491	3.9061	4.0635
C/2	2	3.8023	3.9645	3.9589	4.1138
C/2	2	3.8268	3.9338	3.9213	4.0761
C/2	2	3.8071	3.9168	3.9640	4.1187
C/4	1	3.9107	3.9567	4.0261	3.9914
C/4	1	3.9218	3.9674	4.0255	3.9889
C/4	1	3.9151	3.9615	4.0449	4.0120
C/4	1	3.9076	3.9534	4.0562	4.0198
C/8	0.5	4.0421	4.0300	4.0533	3.9975
C/8	0.5	4.0371	4.0246	4.0802	4.0263
C/8	0.5	4.0389	4.0256	4.0665	4.0096
C/8	0.5	4.0394	4.0264	4.0798	4.0198
C/16	0.25	4.0731	4.0566	4.1271	4.0563
C/16	0.25	4.0885	4.0722	4.0939	4.0268
C/16	0.25	4.0781	4.0610	4.1181	4.0454
C/16	0.25	4.0903	4.0741	4.1077	4.0364
C/32	0.125	4.0269	4.0369	4.1147	4.0355
C/32	0.125	4.0446	4.0542	4.1284	4.0508
C/32	0.125	4.0543	4.0649	4.1337	4.0540
C/32	0.125	4.0359	4.0467	4.1236	4.0461
C/64	0.0625	4.1123	4.0974	4.1871	4.0976
C/64	0.0625	4.1060	4.0898	4.1112	4.0246
C/64	0.0625	4.1201	4.1052	4.1519	4.0676
C/64	0.0625	4.1077	4.0906	4.1572	4.0650
C/128	0.0312	4.1144	4.1103	4.1562	4.1280
C/128	0.0312	4.1318	4.1283	4.1335	4.1094
C/128	0.0312	4.1216	4.1196	4.1293	4.1059
C/128	0.0312	4.1314	4.1293	4.1483	4.1224

Table 3.8: Average charge and discharge capacity for both approaches

C-Rate	$Q_{cavg}$ (Ah)	$Q_{coavg}$ (Ah)	$Q_{davg}$ (Ah)	$Q_{doavg}$ (Ah)
$C/2$	3.8056	3.9376	3.9411	4.0930
$C/4$	3.9138	4.0381	3.9598	4.0030
$C/8$	4.0394	4.0699	4.0266	4.0140
$C/16$	4.0825	4.1117	4.0660	4.0412
$C/32$	4.0404	4.1251	4.0507	4.0466
$C/64$	4.1115	4.1581	4.0957	4.0637
$C/128$	4.1248	4.1481	4.1219	4.1164

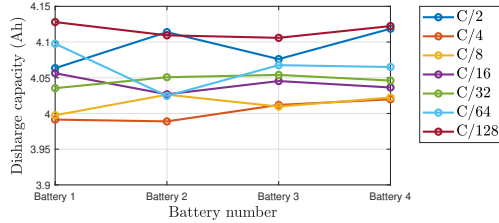


(a) Charge Capacity (offset)

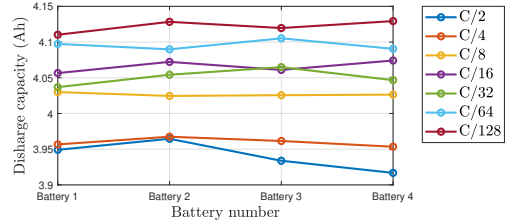


(b) Charge Capacity (non-offset)

Figure 3.17: Charge Capacity Comparison

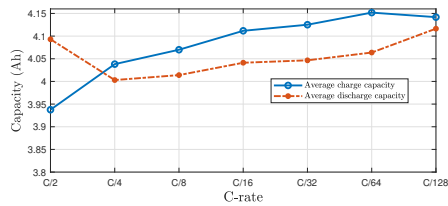


(a) Discharge Capacity (offset)

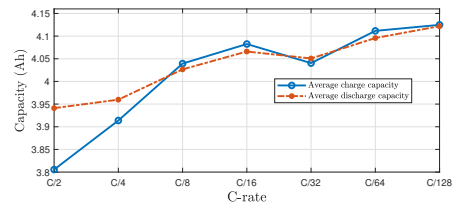


(b) Discharge Capacity (non-offset)

Figure 3.18: Discharge Capacity Comparison



(a) Charge and Discharge Capacity with offset



(b) Charge and Discharge capacity without offset

Figure 3.19: Charge and Discharge Capacity visual for both cases

## 3.9 Conclusions

This thesis presents a comparison analysis for accurate capacity estimation for li-ion batteries with an emphasis to find a more accurate representation capacity of any battery. A voltage difference approach to over-charge and over-discharge the battery was used to offset the voltage drop observed in a battery due to its internal resistance and the charging rate. The proposed approach was tested and compared to other approaches and charging algorithms, and an increase in charge capacity was observed. It followed our hypothesis of an overall increased capacity and an more accurate value of the battery was calculated. Additionally, minimal differences at the low SOC regions due to the volatility of the battery in these low SOC regions were observed. Future work that can be considered is testing on a different variety of chemistry's in batteries to ensure accuracy of the algorithm on different types of batteries. This will allow for a more in-depth look into the accuracy of the capacity of any given battery. Additionally, other work would be to monitor temperature of these batteries to provide us with insights on the effects of the over charge and discharge on the battery over time. These insights will allow us to further improve the algorithm and allow a method to obtain an accurate representation of the capacity of any battery to obtain a more accurate SOC to reduce variations in battery management systems.

## 3.10 Bibliography

- [1] R. Korthauer, *Lithium-ion batteries: basics and applications*. Springer, 2018.
- [2] Y. Wang, J. Tian, Z. Sun, L. Wang, R. Xu, M. Li, and Z. Chen, "A comprehensive review of battery modeling and state estimation approaches for advanced battery management systems," *Renewable and Sustainable Energy Reviews*, vol. 131, p. 110015, 2020.

- [3] G. Dong, Y. Xu, and Z. Wei, “A Hierarchical Approach for Finite-Time High-Infidelity State-of-Charge Observer and Probabilistic Lifetime Prediction of Lithium-Ion Batteries,” *IEEE Transactions on Energy Conversion*, vol. 37, no. 1, pp. 718–728, 2022.
- [4] K. Yu, H. Wang, L. Mao, Q. He, and Q. Wu, “Ic curve-based lithium-ion battery soc estimation at high rate charging current,” *IEEE Transactions on Instrumentation and Measurement*, vol. 71, pp. 1–9, 2022.
- [5] K. Movassagh, A. Raihan, B. Balasingam, and K. Pattipati, “A critical look at coulomb counting approach for state of charge estimation in batteries,” *Energies*, vol. 14, no. 14, 2021.
- [6] M. Petzl and M. A. Danzer, “Advancements in OCV measurement and analysis for lithium-ion batteries,” *IEEE Transactions on Energy Conversion*, vol. 28, no. 3, pp. 675–681, 2013.
- [7] H. Movahedi, N. Tian, H. Fang, and R. Rajamani, “Hysteresis compensation and nonlinear observer design for state-of-charge estimation using a nonlinear double-capacitor li-ion battery model,” *IEEE/ASME Transactions on Mechatronics*, 2021.
- [8] X. Wu, Z. Cui, G. Zhou, T. Wen, F. Hu, J. Du, and M. Ouyang, “Comprehensive early warning strategies based on consistency deviation of thermal–electrical characteristics for energy storage grid,” *Iscience*, vol. 24, no. 9, p. 103058, 2021.
- [9] P. Pillai, J. Nguyen, and B. Balasingam, “Performance analysis of empirical open-circuit voltage modeling in lithium-ion batteries, part-3: Experimental results,” *IEEE Transactions on Transportation Electrification (submitted)*.
- [10] “Safety Data Sheet.” <http://www.molicel.com/wp-content/uploads/00058ar-Molicel-SDS-Y2020.pdf>, 2019. Accessed: 2023-4-18.

# Chapter 4

## Thesis Conclusion

The need for battery characterization and estimation is at an all time high with the increase in use of batteries. This means highest accuracy and faster estimations are critical to continue development and drive the battery industry in a positive direction. In this thesis, we presented an approach to fast OCV characterization to cut the time to characterize any battery to 1/5th of the time. This will reduce the characterization time needed to characterize any battery and allow for more robust testing on reused batteries. This approach utilizes high charging and discharging rates to obtain the fast characterization needed. Next, we explored the voltage drop that occurs when charging and discharging. To counteract this, a voltage offset is applied to obtain the a closer representation of the charge and discharge capacity of the battery. This offset is needed due to the internal resistance as well as effects that come from hysteresis. Future works would be to apply the fast charge algorithm on batteries with different capacities/ different chemistry's to obtain a wider set of data. Additionally, testing the voltage offset and fast charge algorithm while monitoring temperature will allow for an analysis on battery health while testing.

# Vita Auctoris

NAME: James Nguyen

PLACE OF BIRTH: Windsor, ON, Canada

YEAR OF BIRTH: 1999

EDUCATION:

University of Windsor  
Windsor, ON, Canada  
2017-2021, Undergraduate  
Electrical Engineering

University of Windsor,  
Windsor ON, Canada  
2021-2023, Master of Applied Science  
Electrical Engineering